

See discussions, stats, and author profiles for this publication at: <https://www.researchgate.net/publication/238626947>

# Polymorphism of poly(vinylidene fluoride). III. The crystal structure of phase II

ARTICLE *in* MACROMOLECULES · SEPTEMBER 1980

Impact Factor: 5.8 · DOI: 10.1021/ma60077a029

---

CITATIONS

98

---

READS

66

# The Crystal Structure of the $\gamma$ Phase of Poly(vinylidene fluoride)

S. Weinhold, M. H. Litt, and J. B. Lando\*

Department of Macromolecular Science, Case Institute of Technology, Case Western Reserve University, Cleveland, Ohio 44106. Received January 18, 1980

**ABSTRACT:** The crystal structure of the  $\gamma$  phase of poly(vinylidene fluoride) (PVF<sub>2</sub>) was determined by X-ray diffraction techniques. Oriented specimens of the  $\gamma$  phase were obtained by high-temperature drawing of films of ultrahigh molecular weight PVF<sub>2</sub> cast from dimethylacetamide solution. The unit cell of the  $\gamma$  phase was found to be orthorhombic with dimensions  $a = 0.497$ ,  $b = 0.966$ , and  $c = 0.918$  nm. The chain conformation is approximately TTTGTTTG'. Individual chains with this conformation possess a net electrical dipole and pack such that the unit cell is polar. The chains pack in a statistical parallel-antiparallel manner, which can be modeled by a hypothetical four-chain unit cell belonging to space group C2cm.

Four crystal forms of poly(vinylidene fluoride) are known. The  $\alpha$  phase, or phase II, is the form produced by crystallization from the melt at atmospheric pressure<sup>1</sup> at normal degrees of supercooling.<sup>2</sup> The chain conformation of the  $\alpha$  phase has been shown<sup>3,4</sup> to be approximately trans-gauche-trans-gauche'. The unit cell has been reported as being monoclinic<sup>3,4</sup> (or triclinic<sup>4</sup>) with all unit cell angles equal to 90°, within experimental error, and with cell dimensions of  $a = 0.496$ ,  $b = 0.964$ , and  $c = 0.462$  nm. While individual chains of the  $\alpha$  phase possess a net electrical dipole, the two chains in the unit cell pack such that their dipoles exactly cancel, resulting in a nonpolar unit cell.

Several authors<sup>5-7</sup> have recently reported evidence suggesting the existence of a polar version of the  $\alpha$  phase, which is produced by subjecting a film of  $\alpha$ -PVF<sub>2</sub> to a moderately strong poling field. While no detailed structure analysis of this form has been published, it is generally believed that the chain conformation and the unit cell dimensions are similar to that of the  $\alpha$  phase and that the two chains in the cell pack such that their dipoles reinforce rather than cancel one another.

The third known polymorph of PVF<sub>2</sub> is known as the  $\beta$  phase, or phase I. It is most commonly prepared by relatively low temperature mechanical deformation of the  $\alpha$  phase.<sup>1,8</sup> The  $\beta$  phase has been shown<sup>1,3</sup> to consist of planar (or nearly planar) zigzag chains packed into an orthorhombic unit cell with dimensions  $a = 0.858$ ,  $b = 0.491$ , and  $c = 0.256$  nm.

The last known polymorph of PVF<sub>2</sub> is known as the  $\gamma$  phase, or phase III. The techniques which have been reported to yield this crystal phase include the following: crystallization from the melt at high temperatures and pressures;<sup>8,9</sup> annealing the  $\alpha$  phase at high temperatures and pressures;<sup>8</sup> various atmospheric-pressure thermal treatments of both the  $\alpha$ <sup>2,10,11</sup> and  $\beta$ <sup>10</sup> phases; high-temperature crystallization from the melt at atmospheric pressure;<sup>12</sup> and crystallization from dimethyl sulfoxide, dimethylacetamide (DMA), and dimethylformamide solutions.<sup>13-15</sup>

The  $\gamma$  phase very readily undergoes a crystal-crystal phase transition to the  $\beta$  phase when mechanically deformed.<sup>2,8,9</sup> Thus, Hasegawa et al.<sup>3</sup> used unoriented samples to determine their proposed structure for the  $\gamma$  phase. According to Hasegawa et al.,<sup>3</sup> the  $\gamma$ -phase chain conformation is identical with that in the  $\beta$  phase, that is, a nearly all-trans backbone. However, it was proposed that the interchain packing is slightly different in the two crystal phases, resulting in a monoclinic unit cell for the  $\gamma$  phase with dimensions  $a = 0.866$ ,  $b = 0.493$ , and  $c = 0.258$  nm

with the monoclinic angle  $\beta = 97^\circ$ .

In a previous publication<sup>16</sup> we reported a different unit cell for the  $\gamma$  phase of PVF<sub>2</sub>. On the basis of X-ray fiber diffraction patterns, we determined that the unit cell of  $\gamma$ -PVF<sub>2</sub> was orthorhombic with dimensions  $a = 0.497$ ,  $b = 0.966$ , and  $c$  (chain direction) = 0.918 nm. We noted that the  $c$ -axis repeat distance was incompatible with the essentially all-trans chain conformation proposed by Hasegawa et al.<sup>3</sup> This unit cell has since been confirmed by electron diffraction experiments performed with high-temperature melt-crystallized  $\gamma$ -PVF<sub>2</sub>.<sup>12</sup> Also, a detailed infrared study<sup>17</sup> has shown that the crystalline IR spectrum of  $\gamma$ -PVF<sub>2</sub> is much more complicated than was previously believed and has thus demonstrated that the chain conformation cannot be essentially all trans. In addition, a conformational energy analysis has been performed<sup>18,19</sup> with the goal of predicting the major features of the chain conformation of the  $\gamma$  phase.

In this paper we discuss the crystal structure of the  $\gamma$  phase of PVF<sub>2</sub> as determined by X-ray diffraction techniques.

## Experimental Section

**Specimen Preparation.** The preparation of uniaxially oriented films of  $\gamma$ -PVF<sub>2</sub> has been discussed in a previous paper.<sup>16</sup> However, a brief review is in order here. The PVF<sub>2</sub> used for this work was synthesized in our laboratory by a bulk polymerization at 0 °C initiated by <sup>60</sup>Co  $\gamma$  radiation. A detailed discussion of this synthesis technique is to be published.<sup>20</sup> The viscosity of this polymer was measured in DMA at 25 °C with an Ubbelohde dilution viscometer. The intrinsic viscosity  $[\eta]$  was determined to be 8.3 dL/g. The equation<sup>21</sup>  $[\eta] = 1.93 \times 10^{-4} M^{0.677}$  was used in calculating the viscosity-average molecular weight as about  $7 \times 10^6$ . This value for the molecular weight must be considered as only a rough estimate, as  $[\eta]$  is outside the range for which the molecular weight-viscosity relationship was determined. Thin films of  $\gamma$ -PVF<sub>2</sub> were made by casting a DMA solution of this material onto glass plates. Oriented specimens were prepared by drawing these solution-crystallized films at 178 °C. Infrared spectra of the drawn films showed that they consisted predominantly of the  $\gamma$ -phase, but with a significant quantity of the  $\beta$ -phase also present.

**X-ray Techniques.** X-ray fiber diffraction photographs were taken with nickel-filtered Cu K $\alpha$  radiation. A flat-plate camera was used to record the relatively low angle portion of the diffraction pattern, while a cylindrical camera with a diameter of 57.3 mm was used to record diffraction data occurring at larger angles. The cameras were purged with helium to minimize air scattering. The  $d$  spacings were calibrated by dusting the sample with CaF<sub>2</sub>. Multiple film techniques were used for intensity measurements. The relative intensities of the diffraction maxima were measured by scanning the diffraction photographs with a Photometrics microdensitometer and storing the optical density

data on magnetic tape. These data were then computer processed to yield a large two-dimensional optical density matrix from which values for integrated spot intensity and background intensity could be determined. Also, a small amount of data was collected by taking radial densitometer scans of powder diffraction photographs. In addition the intensities of a number of spots, for the most part occurring at large diffraction angles, were determined visually. Corrections for Lorentz and polarization effects were applied. Absorption effects were calculated to be insignificant with respect to the probable error associated with the intensity data; therefore absorption corrections were not applied.

Finally, the effects of the significant quantity of the  $\beta$  phase present in all of the oriented specimens was taken into account. This was necessary because a number of  $\gamma$ -phase and  $\beta$ -phase  $hk0$  reflections overlap. Assuming that the two crystal phases exist in crystallographically separate domains, the relative quantity of the  $\beta$  phase was determined from the intensity of the  $\beta$ -phase 201, 111 and 330, 600 spots. These two spots were chosen because overlap with a  $\gamma$ -phase spot is not possible. The  $\beta$ -phase contribution was then subtracted from the total intensity of overlapping spots, using the observed relative intensities for the  $\beta$  phase reported by Hasegawa et al.<sup>3</sup>

### Refinement Methods

This structure was refined by using the LALS (linked-atom least-squares) mark 6 computer refinement program, which has been developed and described by Smith and Arnott.<sup>22</sup> The use of LALS makes possible the refinement of bond angles, internal rotation angles, intermolecular packing parameters, and scale and isotropic temperature factors. As in any structure refinement routine, LALS bases the structure refinement on observed structure factor amplitudes; however, undesirably short nonbonded interatomic contacts are also considered in the refinement. In addition, bond angles and internal rotation angles can be refined against the restraint that they be stereochemically reasonable.

The structure under discussion was determined in the following general manner. Because the fiber repeat distance is relatively large, a number of stereochemically reasonable chain conformations were possible. To determine which conformation was the correct one, a trial model for each conformation was treated as a rigid body and the interchain packing was refined within the constraints imposed by the known symmetry. This was followed by a limited refinement of bond and internal rotation angles. A full refinement of the most promising conformation was then carried out.

The structure refinement is discussed in terms of the residuals

$$R' = \frac{\sum_{m=1}^M w_m^{1/2} ||F_m(\text{obsd})| - |F_m(\text{calcd})||}{\sum_{m=1}^M w_m^{1/2} |F_m(\text{obsd})|}$$

$$R'' = \left[ \frac{\sum_{m=1}^M w_m ||F_m(\text{obsd})| - |F_m(\text{calcd})||^2}{\sum_{m=1}^M w_m |F_m^2(\text{obsd})|} \right]^{1/2}$$

where  $F_m(\text{obsd})$  and  $F_m(\text{calcd})$  are, respectively, the observed and calculated structure factor amplitudes for the  $m$ th of  $M$  reflections and  $w_m$  is a weighting factor.  $R''$  is the more statistically meaningful of the two residuals and the bulk of the refinement was based upon this quantity. However, most of the residuals reported in the literature are  $R'$ , so this quantity is reported here as well.

For this work the residuals are reported with  $w = 1$  for all reflections; however, it was found that assigning a greater weight to those reflections for which  $\Delta F/F(\text{obsd})$  was large often accelerated the refinement, so this was sometimes done.

Unobserved reflections, also known as less-thans, are those reflections which are not systematically absent because of the symmetry of the structure but are too weak with respect to the background intensity to be observed on the X-ray photograph. The unobserved data were, for the most part, not used in the actual refinement of this structure because of the extreme difficulty in determining an accurate threshold intensity, which varies from place to place on the diffraction photograph. The only

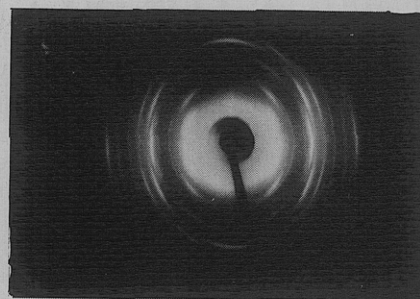


Figure 1. X-ray diffraction pattern of oriented  $\gamma$ -phase PVF<sub>2</sub>.

Table I  
Comparison between Observed and Calculated  
 $d$  Spacings of the  $\gamma$  Phase of PVF<sub>2</sub>

$d_{\text{obsd}}$ , nm	$d_{\text{calcd}}$ , <sup>a</sup> nm	$hkl$	$d_{\text{obsd}}$ , nm	$d_{\text{calcd}}$ , <sup>a</sup> nm	$hkl$
0.480	0.483	020		0.106	370
0.442	0.442	110	0.106	0.105	190
0.271	0.270	130		0.105	371
0.248	0.248 <sub>s</sub>	200	0.431	0.427	021
	0.180	150	0.395	0.398	111
0.176	0.177	151	0.258	0.259	131
	0.173	240	0.336	0.333	022
	0.163	310		0.233	132
0.162	0.161	060	0.237	0.240	201
	0.161	311		0.234	041
	0.159	061		0.214	042
	0.135	260	0.214	0.215	221
0.132	0.134	261	0.168	0.168	152
	0.133	170		0.170	241
	0.132	171	0.160	0.162	242
	0.121	080	0.260	0.259	023
0.120	0.120	420	0.230	0.229 <sub>s</sub>	004
	0.120	081	0.201	0.204	114
	0.119	421			
	0.110 <sub>s</sub>	440			
0.109	0.110	441			
	0.109	280			
	0.108	281			
	0.107 <sub>4</sub>	442			

<sup>a</sup> Spacings calculated from the unit cell of the  $\gamma$  phase of PVF<sub>2</sub> ( $a = 0.497$ ,  $b = 0.966$ , and  $c = 0.918$  nm).

circumstance in which an unobserved reflection was used in the refinement was when the calculated intensity of that reflection was great enough to leave little doubt that if that reflection were indeed the intense, it would be observable. In such a case the unobserved reflection was treated precisely the same as an observed reflection with an observed intensity equal to the threshold value. The unobserved data were, however, of very great importance in choosing between different models for the structure.

LALS is capable of calculating structure factors only for reflections with  $d \geq 0.125$  nm. Hence, several observed reflections with spacing less than this limit were not used in refining the structure. The structure factors for these reflections, as well as those of unobserved reflections with spacings between 0.125 and 0.100 nm, were calculated with a different computer program, using the refined atomic coordinates supplied by LALS.

### Structure Analysis and Results

A fiber diffraction photograph of the  $\gamma$  phase of PVF<sub>2</sub> is shown in Figure 1. Reflections due to the significant amount of  $\beta$  phase in the specimen are also present. In addition, several reflections due to CaF<sub>2</sub> are visible. The  $d$  spacings of the reflections attributed to the  $\gamma$  phase are shown in Table I and are indexed using an orthorhombic unit cell with dimensions  $a = 0.497$ ,  $b = 0.966$ , and  $c$  (chain direction) = 0.918 nm. Due to the rather large  $c$  repeat distance and the imperfect orientation, it is impossible in several cases to resolve reflections on adjacent layer lines with very similar  $d$  spacings. These sets of reflections were

treated as overlapping reflections throughout the refinement.

The dimensions of the  $a$  and  $b$  axes, which are virtually identical with those of the  $\alpha$  phase, indicate that a unit cell contains two chains. The length of the  $c$  axis, which is just slightly less than twice the length of the  $\alpha$ -phase  $c$  axis, and the presence of a strong 004 reflection on the diffraction photograph show that the unit cell contains eight monomer units in the two chains. The calculated crystalline density is  $1.92_8 \text{ g/cm}^3$ , which is essentially identical with the calculated density of the  $\alpha$  phase.

All of the observed reflections can be indexed such that the sum of the  $h$  and  $k$  indices is evenly divisible by 2; this is the condition for a  $C$ -centered unit cell. However, many of the upper layer reflections could also be indexed such that the above condition was not true, while almost none of the  $hk0$  reflections could be indexed such that  $h + k = \text{odd}$ . Thus, there was a possibility that the operative symmetry operation was an  $n$  glide normal to the  $c$  axis rather than  $C$  centering.

Either of these symmetry operations require that, if an atom on one chain exists at a position  $x, y$  in the unit cell, an identical atom on the other chain must exist at position  $x + 1/2, y + 1/2$ . Also, in physical terms a  $C$ -centered structure would mean that the two chains in the unit cell were of the same sense, that is, parallel. On the other hand, an  $n$  glide normal to  $c$  would require the two chains to be antiparallel.

The presence of either of these symmetry elements makes it highly probable, but not absolutely necessary, that a  $c$  glide normal to the  $b$  axis is also present. Only two chain conformations exist which are consistent with a  $c$  glide normal to  $b$  and which can be made to have the proper repeat distance. These conformations are those which have backbone internal rotation angle sequences of TTTGTTTG' or TGTGTG'TG'. The fact that the  $a$  and  $b$  dimensions of the  $\gamma$ -phase unit cell are essentially identical with those of the  $\alpha$  phase indicates that the chain conformation of the  $\gamma$  phase must be such that the interchain packing is very similar to that in the  $\alpha$  phase. This consideration favors the TTTGTTTG' conformation. Also, an infrared study of the  $\gamma$  phase performed by Bachmann et al.<sup>17</sup> favors this conformation as well. Finally, conformational energy calculations<sup>18,19</sup> also point to this conformation.

The conformations investigated in this work included the two mentioned above, TTTGTTTG' and TGTGTG'TG', as well as a third conformation with internal rotation angles of TTTTGTG'. Other possible conformations were not considered here because the conformational energy calculations<sup>18,19</sup> showed them to be quite unfavorable.

In the course of the structure determination, it was found that neither the TGTGTG'TG' conformation nor the TTTTGTG' conformation could be refined to give an acceptably low residual. They were therefore discarded as possibilities. The same was true of two parallel chains with a TTTGTTTG' conformation. A structure consisting of antiparallel chains with such a conformation could be refined to give an acceptably low residual  $R'$  of about 0.18, calculated using only the observed reflections. However, for this model the intensities of a large number of experimentally unobserved reflections were calculated to be quite large. For example, the intensities of several unobserved reflections were calculated to be about 40 times that of the estimated threshold intensity. This drastic disagreement required that the model be discarded as a possibility.

Table II  
Atomic Coordinates of the  $\gamma$  Phase of PVF<sub>2</sub>

atom <sup>a</sup>	$x/a$	$y/b$	$z/c$
C <sub>2</sub>	0.493	0.505	0.862
C <sub>3</sub>	0.549	0.371	0.777
C <sub>4</sub>	0.451	0.372	0.618
C <sub>5</sub>	0.544	0.498	0.528
F <sub>3</sub>	0.442	0.254	0.830
F <sub>4</sub>	0.811	0.339	0.770
F <sub>5</sub>	0.431	0.618	0.569
F <sub>6</sub>	0.809	0.521	0.538
H <sub>1</sub>	0.617	0.584	0.810
H <sub>2</sub>	0.286	0.530	0.833
H <sub>3</sub>	0.515	0.282	0.555
H <sub>4</sub>	0.233	0.371	0.606

<sup>a</sup> Numbering of atoms is shown in Figure 2.

Table III  
Molecular Dimensions of the  $\gamma$  Phase of PVF<sub>2</sub>

Bond Lengths (nm)			
all C-C	0.154	all C-H	0.109
all C-F	0.134		
Bond Angles (Deg)			
C <sub>1</sub> -C <sub>2</sub> -C <sub>3</sub> <sup>a</sup>	117.3	C <sub>1</sub> -C <sub>2</sub> -H <sub>1</sub>	110.6
C <sub>2</sub> -C <sub>3</sub> -C <sub>4</sub>	114.7	C <sub>1</sub> -C <sub>2</sub> -H <sub>2</sub>	113.5
C <sub>3</sub> -C <sub>4</sub> -C <sub>5</sub>	115.0	C <sub>3</sub> -C <sub>4</sub> -H <sub>3</sub>	114.0
C <sub>4</sub> -C <sub>5</sub> -C <sub>6</sub>	118.0	C <sub>3</sub> -C <sub>4</sub> -H <sub>4</sub>	114.0
C <sub>2</sub> -C <sub>3</sub> -F <sub>3</sub>	117.1	F <sub>3</sub> -C <sub>3</sub> -F <sub>4</sub>	102.2
C <sub>2</sub> -C <sub>3</sub> -F <sub>4</sub>	113.3	F <sub>3</sub> -C <sub>3</sub> -F <sub>5</sub>	104.1
C <sub>4</sub> -C <sub>5</sub> -F <sub>5</sub>	114.1	H <sub>1</sub> -C <sub>2</sub> -H <sub>2</sub>	105.7
C <sub>4</sub> -C <sub>5</sub> -F <sub>6</sub>	112.9	H <sub>3</sub> -C <sub>4</sub> -H <sub>4</sub>	103.5
Internal Rotation Angles (Deg)			
C <sub>1</sub> -C <sub>2</sub> -C <sub>3</sub> -C <sub>4</sub>	170.4	C <sub>3</sub> -C <sub>4</sub> -C <sub>5</sub> -F <sub>5</sub>	-68.9
C <sub>2</sub> -C <sub>3</sub> -C <sub>4</sub> -C <sub>5</sub>	51.5	C <sub>3</sub> -C <sub>4</sub> -C <sub>5</sub> -F <sub>6</sub>	49.7
C <sub>3</sub> -C <sub>4</sub> -C <sub>5</sub> -C <sub>6</sub>	170.4	C <sub>2</sub> -C <sub>3</sub> -C <sub>4</sub> -H <sub>3</sub>	172.2
C <sub>4</sub> -C <sub>5</sub> -C <sub>6</sub> -C <sub>7</sub>	171.5	C <sub>2</sub> -C <sub>3</sub> -C <sub>4</sub> -H <sub>4</sub>	-69.3
C <sub>1</sub> -C <sub>2</sub> -C <sub>3</sub> -F <sub>3</sub>	49.7	C <sub>4</sub> -C <sub>5</sub> -C <sub>6</sub> -H <sub>5</sub>	-67.8
C <sub>1</sub> -C <sub>2</sub> -C <sub>3</sub> -F <sub>4</sub>	-68.9	C <sub>4</sub> -C <sub>5</sub> -C <sub>6</sub> -H <sub>6</sub>	50.8

<sup>a</sup> Numbering of atoms is shown in Figure 2.

On the basis of this knowledge, the structure of the  $\gamma$  phase was ultimately determined to consist of chains with a TTTGTTTG' conformation packed in a statistical parallel-antiparallel manner. The occurrence of statistical packing in semicrystalline polymers is well established. In statistical parallel-antiparallel packing, the two chains in any given unit cell are either parallel or antiparallel, but different unit cells within the same crystallite may have either type of packing. For computational purposes this may be modeled by assuming a hypothetical unit cell in which two fractionally weighted chains, one of each sense, are placed at each chain position in the unit cell. For this work it was assumed that parallel packing and antiparallel packing occur with equal probability. Hence, this structure is modeled as a unit cell containing two up chains and two down chains, with the scattering factor for each atom divided by a factor of 2.

On the basis of zero-layer X-ray data, which are not dependent on the sense of the chains, it was determined that the TTTGTTTG' conformation was the only possibility. A refinement of the chain conformation and the interchain packing was performed.

The atomic coordinates of an asymmetric unit, which consists of two monomer units, are given in Table II. Details of an individual chain with the numbering of the atoms indicated is shown in Figure 2. All intrachain, nonbonded atomic distances less than the sum of the van der Waals radii of the two atoms are also shown in Figure 2a. The van der Waals radius of a fluorine atom is taken to be 0.135 nm, while that of a hydrogen atom is taken as

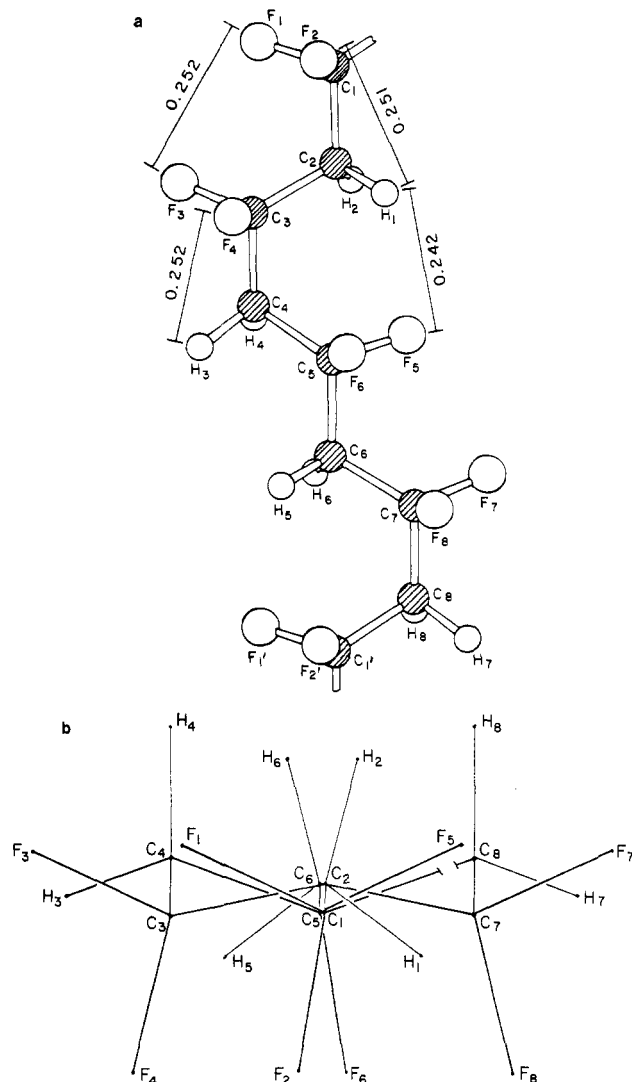


**Figure 2.** A single chain in the  $\gamma$ -phase conformation: (a)  $bc$  projection; (b)  $ab$  projection. Distances shown are in nm.

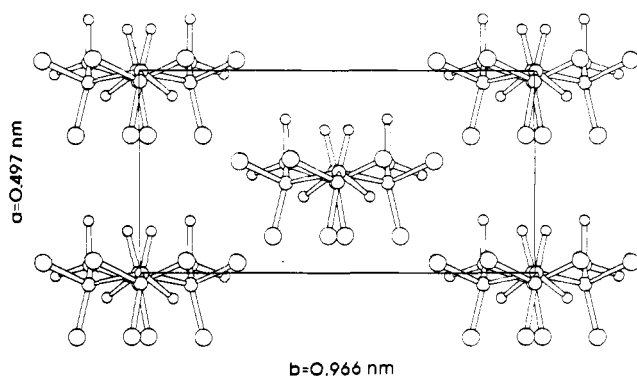


**Figure 3.**  $ab$  projection of the structure of the  $\gamma$  phase of  $\text{PVF}_2$ .

0.120 nm. The worst contact is between two fluorine atoms in the trans segment of the chain. The distance of 0.252 nm is quite close, but not bad enough to dismiss the possibility of its occurring. The molecular dimensions of this chain are given in Table III. Backbone bond angles range from about  $115^\circ$  to  $118^\circ$ , while trans backbone internal rotation angles are about  $170^\circ$  and the gauche angle is about  $52^\circ$ . An estimate of the degree of uncertainty associated with these parameters is  $\pm 1^\circ$  for the bond angles and probably somewhat more than this for the rotation angles. Uncertainty estimates given for this work are in

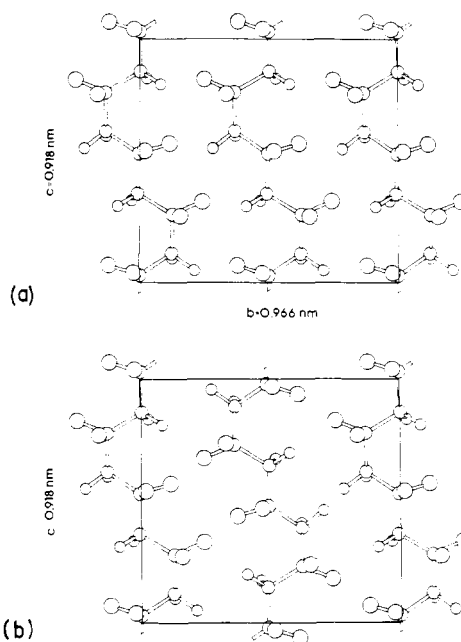


**Figure 4.**  $bc$  projections of the structure of the  $\gamma$  phase of  $\text{PVF}_2$  demonstrating the packing of (a) parallel chains and (b) antiparallel chains.

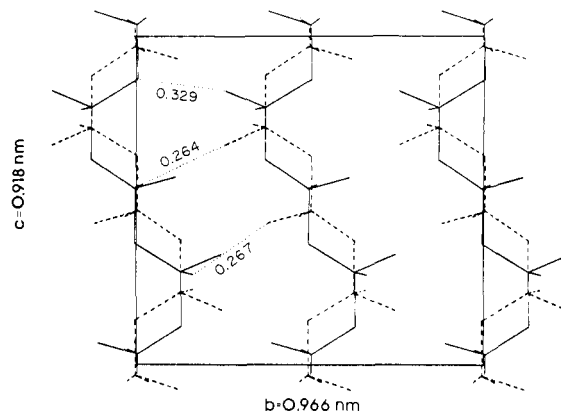


**Figure 5.** Sketch of the  $bc$  projection of the hypothetical four-chain unit cell used to model the structure of the  $\gamma$  phase of  $\text{PVF}_2$ . Solid lines illustrate chains with one sense and dashed lines illustrate chains with the opposite sense. Distances shown are in nm.

no way well-defined mathematical quantities. They are included to give some indication of the range in value which a parameter may adopt without serious detriment to the X-ray residuals and/or nonbonded interatomic contacts.

An  $ab$  projection of the structure is shown in Figure 3. Because the atoms of the two chains of opposite sense at the same position in the unit cell exactly overlap in this projection, only two chains are evident. Figure 4 shows the  $bc$  projections of parallel and antiparallel chains. Figure 5 shows a sketch of the  $bc$  projection of the cell with up and down chains at each position. Hydrogen atoms have been omitted for clarity. The dotted lines point out the three close interchain contacts. Taking the van der Waals radius of a fluorine atom to be 0.135 nm and that of a methylene group to be 0.200 nm, the closest contact is 0.006 nm short of the sum of the van der Waals radii, a relatively insignificant amount.

We have chosen to define the interchain packing as we have because of the very high symmetry of the resulting structure. The space group for this hypothetical four-chain unit cell structure is  $C2cm$  (No. 40<sup>23</sup>). All four chains are



Table IV  
Comparison between Observed and Calculated  
Structure Factor Amplitudes of the  $\gamma$  Phase of PVF<sub>2</sub>

$hkl^a$	$ F_o ^b$	$ F_c ^c$	$hkl$	$ F_o $	$ F_c $
020	38.1	36.9	442		
110	very strong <sup>d</sup>	175.0	280	74.8	70.9
021			441		
130			440		
200	108.3	97.9	281		
151	74.9	85.3	190	52.6	43.7
150			370		
240			371		
310	114.1	108.9	111	81.3	89.6
311			131	55.4	55.7
060			022	122.2	122.4
061			132	183.8	143.2
171			041		
170			201		
260	63.7	56.8	042	102.8	44.4
261			221		
080			152		
421	70.0	62.6	241	42.3	50.0
420			242	43.5	46.2
081			023	78.8	89.0
			114	32.5	83.4

<sup>a</sup> In the case of overlapping reflections, the planes contributing to that spot are listed such that the plane with the greatest calculated contribution to the intensity of the spot is listed first, the plane with the second greatest calculated contribution is listed second, etc. <sup>b</sup> The observed structure factor amplitude is  $k(I_{\text{obsd}})^{1/2}$ , where  $I_{\text{obsd}}$  is the observed relative intensity and  $k$  is the scale factor. The calculated structure factor amplitude is  $(mF_c^2)^{1/2}$ , where  $m$  is the multiplicity and  $F_c$  is the calculated structure factor. For overlapping reflections this value is  $(\sum mF_c^2)^{1/2}$ . <sup>d</sup> This spot was not considered in the structure refinement; see text.

generated by symmetry from the asymmetric unit consisting of two monomer units. The residual can be slightly decreased by changing the relative shift of the two parallel chains along the  $c$  axis or by slightly rotating the chains about their axes. However, these changes would drastically reduce the symmetry of the structure. The slight decrease in the residual produced by these changes is not statistically significant, considering the additional degrees of freedom made available by reducing the symmetry. Estimates for the uncertainty associated with the packing parameters are as follows:  $\pm 0.005c$  for the relative shift along  $c$  between antiparallel chains,  $\pm 0.03c$  for the shift between parallel chains, and  $\pm 2^\circ$  for the rotation of the chains about a line parallel to the  $c$  axis that might be considered to be the chain axis. As the chains are not helical, they do not possess a precisely defined chain axis.

Table IV lists calculated vs. observed structure factor amplitudes for all of the observed reflections. The calculated values were computed with the overall isotropic temperature factor  $B = 3.75 \text{ \AA}^2$ . The temperature and scale factors were refined parameters and have an estimated uncertainty of  $\pm 0.25 \text{ \AA}^2$  for  $B$  and  $\pm 3\%$  for the scale factor. The 110,021 spot was not considered in the refinement because an accurate determination of its intensity was impossible for two reasons. First, it is the strongest reflection on the diffraction pattern and thus is difficult to scale to weaker spots. The greatest cause of uncertainty, however, was overlap with the very intense  $\beta$ -phase 110,200 spot. Nonetheless, the  $\gamma$ -phase 110,021 reflection has a greater calculated intensity than any other reflection, in agreement with experiment.

For this work, the observed intensity was defined to be the sum of the intensities of all of the spots on the diffraction pattern with the same  $hkl$ . This is contrary to the conventional definition, where the observed intensity is

taken to be the average intensity of one of these spots. It was necessary to define observed intensity in this manner because of the overlap between zero-layer reflections, for which there are two equivalent spots, and first-layer reflections, for which there are four equivalent spots.

The residuals for this structure, based on all the observed data except the 110,021 reflection, are  $R' = 0.174$  and  $R'' = 0.253$ . The agreement for unobserved reflections is also quite good, with only a few unobserved reflections having a calculated intensity greater than the estimated threshold intensity. A residual incorporating unobserved reflections can be calculated by ignoring those reflections with a calculated intensity less than the threshold and treating those reflections with a calculated intensity greater than the threshold as observed reflections with an observed intensity equal to the threshold.

The residual calculated from both the unobserved reflections and the observed reflections (except the 110,021), with unity weight assigned to each reflection, was  $R' = 0.218$ . For comparison, this residual for the nonstatistical, antiparallel-chain model mentioned previously was 0.50.

## Discussion

There exists a considerable body of literature concerned with the high-pressure crystallization of poly(vinylidene fluoride).<sup>8,9,24-27</sup> However, the results of these experiments are confused, with some authors<sup>8,9</sup> reporting the formation of the  $\gamma$  phase and other investigators<sup>24,25</sup> reporting the formation of the  $\alpha$  and/or  $\beta$  phase under similar conditions. As X-ray diffraction was the predominant technique used to identify the crystal phases present in these samples, some of this confusion may be due to the incorrect  $\gamma$ -phase unit cell proposed by Hasegawa et al.<sup>3</sup>

The crystal structure of the  $\gamma$  phase presented here also sheds light on the thermally induced  $\alpha$ -phase to  $\gamma$ -phase transition. It has been shown<sup>2,10,11</sup> that annealing melt-crystallized  $\alpha$ -phase spherulites close to their melting temperature results in a solid-state transition from the  $\alpha$  phase to the  $\gamma$  phase. However, a solid-state transition from the  $\beta$  phase to the  $\gamma$  phase does not occur.<sup>10</sup> This behavior is somewhat difficult to explain if the  $\gamma$  phase is considered to be a minor modification of the  $\beta$  phase, as proposed by Hasegawa et al.<sup>3</sup> On the other hand, this behavior seems quite reasonable in light of the great similarity in the chain packing of the  $\alpha$  phase and the  $\gamma$  phase described in this report.

Similarly, the  $\gamma$ -phase to  $\beta$ -phase solid-state transition, which occurs very readily upon mechanical deformation of the  $\gamma$  phase, would seem to be unlikely if the two phases were composed of chains with the same extended conformation as proposed by Hasegawa et al.<sup>3</sup> However, since it is known that the  $\alpha$  phase undergoes a similar transition to the  $\beta$  phase<sup>1,3,4,8</sup> and since the chain conformation of the  $\gamma$  phase can be taken to be a high-energy intermediate between that of the  $\alpha$  and  $\beta$  phases, the  $\gamma \rightarrow \beta$  transition is quite predictable.

Also, this work poses a question regarding the chain packing in the  $\alpha$  and  $\delta$  (polar  $\alpha$  or phase IV) phases of PVF<sub>2</sub>. We have shown here that statistical parallel-antiparallel chain packing is present in the  $\gamma$  phase. As the  $\alpha$  phase can undergo a solid-state transition to the  $\gamma$  phase, it is possible that statistical parallel-antiparallel packing is also present in the  $\alpha$  phase. This possibility is supported by the work of Doll and Lando,<sup>4</sup> who found that two equally likely structures for the  $\alpha$  phase could be proposed, one with parallel-chain packing and one with antiparallel packing. Of course, if statistical parallel-antiparallel packing is in fact present in the  $\alpha$  phase, one would expect

it to also be present in the  $\delta$  phase.

Finally, it should be recognized that in this structure there is a clear violation of the equivalency postulate,<sup>28</sup> since the asymmetric unit of structure contains two chemically identical monomer units which have different conformations (TT vs. TG).

### Conclusions

The structure of the  $\gamma$  phase of PVF<sub>2</sub> has been determined. The unit cell is orthorhombic with dimensions  $a = 0.497$ ,  $b = 0.966$ , and  $c = 0.918$  nm. The chain conformation is approximately TTTGTTTG'. Individual chains have a net electrical dipole, and the chain packing is such that the unit cell is polar. The chains pack in a statistical parallel-antiparallel manner. The statistical nature of the structure can be modeled with a hypothetical four-chain unit cell belonging to space group  $C2cm$ . The residuals for this structure are  $R' = 0.174$  and  $R'' = 0.253$ .

**Acknowledgment.** This research was supported by the Defense Advanced Research Projects Agency and monitored by the Army Night Vision Laboratory under Contract No. DAAK 70-77-C-0055.

### References and Notes

- (1) J. B. Lando, H. G. Olf, and A. Peterlin, *J. Polym. Sci., Part A-1*, **4**, 941 (1966).
- (2) W. M. Prest, Jr., and D. J. Luca, *J. Appl. Phys.*, **46** (10), 4136 (1975).
- (3) R. Hasegawa, Y. Takahashi, Y. Chatani, and H. Tadokoro, *Polym. J.*, **3** (5), 600 (1972).
- (4) W. W. Doll and J. B. Lando, *J. Macromol. Sci., Phys.*, **B4** (2), 309 (1970).
- (5) G. T. Davis, J. E. McKinney, M. G. Broadhurst, and S. C. Roth, *J. Appl. Phys.*, **49** (10), 4998 (1978).
- (6) D. Naegle, D. Y. Yoon, and M. G. Broadhurst, *Macromolecules*, **11** (6), 1297 (1978).
- (7) G. R. Davies and H. Singh, *Polymer*, **20**, 772 (1979).
- (8) R. Hasegawa, M. Kobayashi, and H. Tadokoro, *Polym. J.*, **3** (5), 591 (1972).
- (9) W. W. Doll and J. B. Lando, *J. Macromol. Sci., Phys.*, **B2** (2), 219 (1968).
- (10) W. M. Prest, Jr., and D. J. Luca, *J. Appl. Phys.*, **49** (10), 5042 (1978).
- (11) S. Osaki and Y. Ishida, *J. Polym. Sci., Polym. Phys. Ed.*, **13**, 1071 (1975).
- (12) A. J. Lovinger and H. D. Keith, *Macromolecules*, **12** (5), 919 (1979).
- (13) G. Cortilli and G. Zerbi, *Spectrochim. Acta, Part A*, **23**, 2216 (1967).
- (14) Ye. L. Gal'Perin, B. P. Kosmynin, and R. A. Bychkov, *Vysokomol. Soedin., Ser. B*, **12**, 555 (1970).
- (15) M. Kobayashi, K. Tashahiro, and H. Tadokoro, *Macromolecules*, **8**, 158 (1975).
- (16) S. Weinhold, M. H. Litt, and J. B. Lando, *J. Polym. Sci., Polym. Lett. Ed.*, **17**, 585 (1979).
- (17) M. A. Bachmann, W. L. Gordon, J. L. Koenig, and J. B. Lando, *J. Appl. Phys.*, **50** (10), 6016 (1979).
- (18) S. K. Tripathy, R. Potenzzone, Jr., A. J. Hopfinger, N. C. Banik, and P. L. Taylor, *Macromolecules*, **12**, 656 (1979).
- (19) N. C. Banik, P. L. Taylor, S. K. Tripathy, and A. J. Hopfinger, *Macromolecules*, **12**, 1015 (1979).
- (20) M. H. Litt, S. Mitra, and J. B. Lando, to be submitted to *Macromolecules*.
- (21) G. J. Welch, *Polymer*, **15**, 429 (1974).
- (22) P. J. C. Smith and S. Arnott, *Acta Crystallogr., Sect. A*, **34**, 3 (1978).
- (23) "International Tables for X-Ray Crystallography", Vol. 1, Kynoch Press, Birmingham, England, 1952, p 126.
- (24) W. W. Doll and J. B. Lando, *J. Macromol. Sci., Phys.*, **B4** (4), 889 (1970).
- (25) K. Matsushige and T. Takemura, *J. Polym. Sci., Polym. Phys. Ed.*, **16**, 921 (1978).
- (26) K. Matsushige, K. Nagata, and T. Takemura, *Jpn. J. Appl. Phys.*, **17** (3), 467 (1978).
- (27) J. Scheinbeim, C. Nakafuku, B. A. Newman, and K. D. Pae, *J. Appl. Phys.*, **50** (6), 4399 (1979).
- (28) G. Natta and P. Corradini, *Nuovo Cimento, Suppl.*, **15**, 9 (1960).

## Packing Analysis of Carbohydrates and Polysaccharides. 11. Molecular and Crystal Structure of Native Ramie Cellulose

Carrie Woodcock and Anatole Sarko\*

Department of Chemistry, State University of New York, College of Environmental Science and Forestry, Syracuse, New York 13210. Received January 9, 1980

**ABSTRACT:** The crystal structure of ramie cellulose I has been determined by an X-ray diffraction analysis combined with stereochemical model refinement. The structure crystallizes in a monoclinic, two-chain unit cell, in which the chain arrangement is parallel and the most likely space group is  $P2_1$ . The conformation of both chains is based on a one glucose residue asymmetric unit, with the hydroxymethyl group tg, and the  $2_1$  screw axis coincident with the chain axis. The chains are hydrogen bonded two dimensionally into sheets arranged along the (200) planes. The sheets are staggered by  $1/4c$  relative to one another and have no hydrogen bonds between them. In these features, the crystal structures of ramie and *Valonia* cellulose are nearly identical. The X-ray reliability index  $R'' = 0.194$ , and the parallel-chain structure is statistically preferred over the best antiparallel structure at a 99.5% significance level.

Previous crystallographic studies of cellulose I of the alga *Valonia ventricosa* have shown that this highly crystalline native cellulose has a parallel-chain structure.<sup>2,3</sup> Other native celluloses, typically those of ramie, cotton, or wood, are, however, less crystalline and may have a unit cell smaller than that of *Valonia* cellulose.<sup>4</sup> As a result, a belief persists that not all native celluloses are identical in crystal structure and that some may be based on an antiparallel-chain lattice. The present study on ramie cellulose was, therefore, undertaken to determine its crystal structure in suitable detail for a comparison with the *Valonia* cellulose. In view of the apparent identity of the diffraction

patterns of ramie and similar celluloses, this study should also have a bearing on the structure of other native celluloses.

### Experimental Procedures

A sample of purified, relatively high crystalline ramie was obtained from Dr. T. E. Timell of this college. The sample was treated with the cellulase of *Pestalotiopsis westerdijkii* QM381 (obtained from Dr. M. Mandels, U.S. Army Natick Research and Development Command, Natick, Mass.) at the optimum conditions for this enzyme<sup>5</sup> in an effort to improve crystallinity further. However, no significant improvement in the resolution of the X-ray diffraction diagrams resulted, except that the faint layer-line